J Porous Mater
DOI 10.1007/s10934-016-0261-5

Zeolite-Y encapsulated VO[2-(2′-hydroxyphenyl)benzimidazole] complex: investigation of its catalytic activity towards oxidation of organic substrates

E. R. Shilpa[1] · V. Gayathri[1] · G. K. Kiran[1]

Abstract Zeolite-Y encapsulated VO(IV)2-(2′-hydroxyphenyl)benzimidazole (ohpbmzl) was synthesized by flexible ligand approach and characterized using various physico-chemical techniques such as elemental analysis, XRD, inductively coupled plasma-atomic emission, fourier transform infrared spectroscopy, UV–vis-diffuse reflectance and electron paramagnetic resonance spectroscopy, thermogravimetric analysis, BET surface area and cyclic voltammetry (CV). Based on the results a square pyramidal structure was suggested for the encapsulated complex. Shift in UV absorbance to higher wavelength and variations in the redox potential values compared to the non-encapsulated complex in CV confirmed the successful encapsulation of the complex in the zeolite matrix. The catalytic efficacy was investigated towards oxidation of phenol, styrene, cyclohexane and ethyl benzene in acetonitrile using H_2O_2 as oxidant. Influence of reaction parameters like catalyst and substrate concentration, substrate/H_2O_2 molar ratio, and temperature were investigated to optimize the reaction conditions for maximum substrate conversion and selectivity towards desired products using the encapsulated complex. The catalytic activity was compared with vanadyl exchanged zeolite-Y (VO-Y) and non-encapsulated complex. The encapsulated complex retained its stability up to 3 runs as confirmed by recycling studies. Mechanistic pathways were proposed for all the probe reactions.

✉ V. Gayathri
gayathritvr@yahoo.co.in

[1] Department of Chemistry, Bangalore University, Central College Campus, Dr. Ambedkar Veedi, Bangalore, Karnataka 560001, India

Keywords Zeolite encapsulated vanadium complex · Electrochemical studies · Oxidation of organic compounds · H_2O_2

1 Introduction

Encapsulation of transition metal complexes, acting as homogeneous catalysts, in the cavity of zeolite offers the advantages of heterogeneous catalysts, share many beneficial features of homogeneous catalysts and curtails the disadvantages of both. The higher selectivity, easy product separation, enhanced yield than the homogeneous and heterogeneous complements has made them to be explored as heterogeneous catalysts in petroleum industries, pharmaceutical applications and fine chemical productions. Several research groups have investigated the catalytic properties of the complexes entrapped within the supercages of zeolite-Y [1–3]. The coordination chemistry of vanadium is of great current interest due to its wide application in medicinal and catalytic systems [4]. Its coordination number and geometry is highly ligand dependent. The majority of vanadium (IV) compounds contain VO^{2+} unit (vanadyl ion) and have square pyramidal or trigonal bipyramidal geometries with an axial oxo ligand. Oxovanadium center can act as Lewis acid towards electron rich species such as peroxides [H_2O_2 or t-butyl hydroperoxide (TBHP)] to form metalloperoxo species, which are proficient in transferring an oxygen atom to a wide range of organic and inorganic substrates [5, 6]. Furthermore, the use of environmentally friendly oxidants like hydrogen peroxide upsurges significantly their potential applications. Hence, these oxovanadium complexes have attracted considerable attention due to their remarkable catalytic activity and have displayed good selectivity for the oxidation of various substrates.

Published online: 25 August 2016

Oxidation of phenol is an industrially important process due to pharmaceutical significance of its products catechol and hydroquinone [7]. Similarly, styrene oxidation holds substantial interest in academic as well as industrial research owing to its imperative products such as styrene oxide, benzaldehyde or phenylacetaldehyde which are otherwise synthesized by using strong oxidants such as peroxyacids, manganese dioxide, chromic acid, potassium dichromate or selenium dioxide, producing large amounts of undesired and/or toxic wastes, most significantly when applied to industrial processes [8–14]. On the other hand, oxidation of cyclohexane to cyclohexanol and cyclohexanone (K/A oil) has achieved much attraction in industries as the two are strategic intermediates in the production of adipic acid (to make Nylon-66) and caprolactam (to make Nylon-6). More importantly, higher selectivity towards cyclohexanone is desirable in a variety of chemical syntheses [11, 12, 15]. Hence, several experiments have been conducted to develop new catalysts so as to assist the oxidation of cyclohexanol under mild conditions with high selectivity for a particular end product by using different oxidizing agents. Correspondingly, oxidation of ethyl benzene to acetophenone has maintained a prominent position in pharmaceutical sector because of its use as an intermediate in the manufacture of pharmaceuticals, perfumes, resins and alcohols [16]. Earlier, synthesis of acetophenone was performed using stoichiometric quantities of oxidizing agents like $KMnO_4$ or $K_2Cr_2O_7$ or via Friedel–Crafts acylation reaction of aromatics by acid halide/anhydride, using stoichiometric amounts of corrosive $AlCl_3$ catalyst. The current industrial production of benzylic ketones is based on the oxidation of alkyl benzenes with molecular oxygen using cobalt acetate as the catalyst in acetic acid [17].

Although encapsulation process is well established in the literature and a variety of complexes are synthesized, still there is always been a demand for more efficient heterogenised homogeneous catalysts. Hence, considering the benefits of zeolite frame work, vanadium and the probe reactions, the present work emphasizes on the encapsulation of the vanadium(IV) complex of 2-(2′-hydroxyphenyl)benzimidazole (ohpbmzl) by flexible ligand method into zeolite-Y. Moreover, encapsulation of $VO(opbmzl)_2$ within the zeolite-Y framework is not reported earlier. Since, redox properties of a catalyst also influence its catalytic activity, electrochemical behavior of the catalyst was studied. The cyclic voltammetric study of encapsulated vanadyl complex of benzimidazole derivative is carried out for the first time in the present case.

The catalytic efficacy of encapsulated $VO(opbmzl)_2Y$ was probed towards the industrially important reactions like oxidation of phenol, styrene, cyclohexane and ethyl benzene and reaction conditions were optimized to obtain maximum product yield.

2 Experimental

2.1 Materials

The commercially available Na-Y zeolite was supplied from Sud-Chemie, India and was used as received without further purification. The other reagents like $VOSO_4.5H_2O$ (Lobo Chemie Pvt. Ltd.), orthophenylenediamine (S.d. fine chem. Ltd., India), diphosphorus pentoxide, orthophosphoric acid, 2,6-di-tert-butyl-4-methylphenol (butylated hydroxytoulene, BHT), salicylic acid, phenol, cyclohexane, ethylbenzene, hydrogen peroxide (H_2O_2) (Merck), tetrabutylammonium bromide (Spectrochem. Pvt. Ltd., India), styrene, tetrabutyl hydroperoxide (TBHP), (Sigma Aldrich) and vulcan carbon (Cabot corporation) were used as received. All the solvents were distilled prior to use.

2.2 Characterization

All the samples were vacuum dried before analysis. The elemental analyses were obtained with an Elementar Vario micro cube CHNS analyzer. The vanadium content was determined using ICP-AES at Atomic Mineral Directorate, Southern region, Bangalore. The surface area and pore volume were measured by BET method using Micromeritics surface area analyzer model ASAP 2020. The XRD patterns were recorded on a Panalytical X'pert Pro MPD powder X-ray diffractometer using Cu Kα radiation ($\lambda = 1.542$ Å) in the 2θ range 10°–80° at a scanning rate of 2°/min. The UV–visible-DRS spectra were recorded using a Shimadzu UV–Vis-NIR model UV-3101P spectrophotometer having an integrating sphere attachment for the solid samples in $BaSO_4$. The IR spectra of the samples were recorded in the range 400–4000 cm^{-1} as KBr disks on a Shimadzu 8400 s FT-IR spectrometer. The ESR spectra were recorded using a Bruker EMX EPR spectrometer X-band, $\nu = 9.431$ GHz at room temperature (Indian Institute of Science, Bangalore). The electrochemical properties were studied by recording the cyclic voltammograms of non-encapsulated and encapsulated complexes on an EG & G Model Versastat IIA Galvanostat/Potentiostat with a digital recorder by using 0.1 M tetrabutylammonium perchlorate (TBAP) as the supporting electrolyte in DMF (dimethylformamide). The working electrode was prepared by taking a 1:1 ratio by weight of non-encapsulated or encapsulated metal complexes in 1 mL of milli Q water which was coated on platinum flag of 8.0 cm^2 area; 2 mL of nafion binder (Sigma Aldrich) was then added on this coating and followed by air drying. The platinum flag electrode and standard calomel electrode (SCE) were used as the working and reference electrodes respectively. The CV of the non-encapsulated complex was

taken both in solid and solution modes, using 0.01 M of the metal complex in DMF. Thermograms (TG) were recorded on a TA instrument under nitrogen atmosphere with heating rate of 20 °C/min from 20 to 1000 °C. All the reaction products were analyzed using a Shimadzu 14B gas chromatograph (GC) fitted with flame ionization detector using a BP-5 capillary column.

2.3 Preparation

2.3.1 Synthesis of zeolite encapsulated VO(IV)2-(2′-hydroxyphenyl)benzimidazole {VO(opbmzl)$_2$}

In a typical experiment, 5 g of Na-Y zeolite was suspended in 300 ml distilled water containing $VOSO_4.5H_2O$ (12.6 g, 50 mmol) and heated at 90 °C under stirring for 48 h. The obtained green coloured solid was filtered, thoroughly washed with hot distilled water and then Soxhlet extracted, till the filtrate was free from vanadyl ions and subsequently dried at 150 °C for 12 h in a hot air oven. The vanadium content in vandyl-exchanged zeolite-Y (VO-Y) was found to be 2.3 % (Table 1). Preparation of the ohpbmzl and the non-encapsulated complex VO(opbmzl)$_2$ is reported elsewhere [18].

VO(opbmzl)$_2$-Y was synthesized by refluxing an ethanolic solution of ohpbmzl and VO(IV) exchanged zeolite-Y at 60 °C for 48 h and the product formed was washed using ethanol followed by THF and acetone by Soxhlet extraction. The uncomplexed VO(IV) ion present in the zeolite-Y was exchanged with Na^+ ions by treating with aqueous 0.1 M NaCl solution, filtered and washed with distilled water and dried at 120 °C for 24 h (Scheme 1). Vanadium content was found to be 1.5 %.

2.3.2 Catalytic activity towards probe reactions

2.3.2.1 Oxidation of phenol In a typical reaction, an aqueous solution of H_2O_2 (30 % w/v, 8.5 g, 75 mmol) and phenol (4.7 g, 50 mmol) were mixed in 6 mL of CH_3CN and the reaction mixture was heated at 60 °C with continuous stirring in an oil bath. The reaction was considered to begin after addition of 0.115 g of catalyst. Aliquots at several intervals were taken and the reaction products were analysed using GC.

2.3.2.2 Oxidation of styrene According to a conventional procedure, styrene (5.2 g; 50 mmol) and 30 % H_2O_2 (11.4 g; 100 mmol) in 10 mL CH_3CN was heated with continuous stirring at 70 °C for 6 h using 0.125 g of catalyst. The progress of the reaction was monitored as mentioned above.

2.3.2.3 Oxidation of cyclohexane In a typical reaction, an aqueous solution of 30 % H_2O_2 (17.0 g, 150 mmol) and cyclohexane (6.3 g, 75 mmol) were mixed in 10 ml of CH_3CN and the reaction mixture was heated at 60 °C with continuous stirring in an oil bath. The reaction was considered to begin after addition of 0.135 g of catalyst and the products were analyzed as stated above.

2.3.2.4 Oxidation of ethyl benzene In a typical reaction, ethylbenzene (5.3 g; 50 mmol) and 30 % H_2O_2 (11.4 g; 100 mmol) in 6 mL CH_3CN was heated with continuous stirring at 60 °C for 6 h using 0.125 g of catalyst. The progress of the reaction was monitored by gas chromatograph by taking aliquots at specific intervals. The influence of external parameters on the catalytic activity of VO(opbmzl)$_2$-Y was studied by varying temperature, catalyst and substrate concentration, substrate: H_2O_2 molar ratio.

3 Results and discussion

Vanadium, carbon and nitrogen content estimated after encapsulation can be assigned to the presence of transition metal complex in the nano-cavities of zeolite-Y. Absence of sulphate in VO exchanged zeolite Y, non-encapsulated and encapsulated complexes was confirmed by elemental analysis. The elemental analysis data of VO(IV) based non-encapsulated, the entrapped complex and VO(IV)

Table 1 Physical and textural properties of catalysts

Catalyst	Colour	Elemental analysis (%)				Textural properties	
		C	H	N	V	Total pore volume (cc/g)	Surface area (m^2/g)
NaY	White	–	–	–	–	0.30	530
VO-Y	Green	–	–	–	2.3	0.27	445
VO(opbmzl)$_2$-Y	Light green	3.0	2.6	0.6	1.5	0.16	224
VO(opbmzl)$_2$	Green	63.1 (63.9)	3.4 (3.8)	10.7 (11.2)	9.9 (10.5)	–	–

* Calculated percentage composition is given in the parenthesis

Scheme 1 Preparation of $VO(opbmzl)_2$-Y

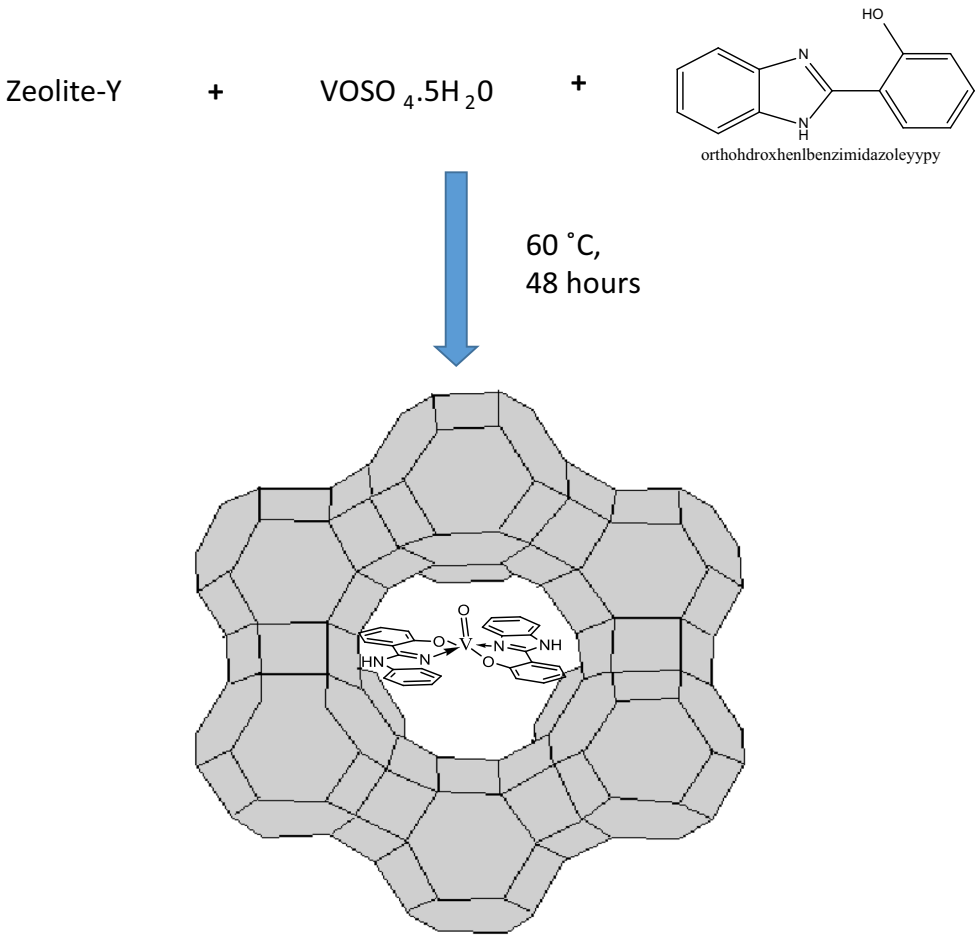

exchanged-Yare tabulated in Table 1 along with the specific surface area and specific pore volume measurement data. The lowering of the pore volume and surface area supported the fact that VO(IV) complexes are present within the zeolite cages and not on the external surface.

Elemental analysis of $VO(opbmzl)_2$-Y indicated that not all VO^{2+} ions have complexed with ohpbmzl, as only VO^{2+} ions present in the super cages of zeolite-Y are available for the complexation, whereas those present in the sodalite cages (diameter $\sim$6.0 Å) and other sites like V, II', III' etc., are unavailable for coordination due to space restriction [19].

3.1 Structural integrity studies

The powdered XRD patterns of NaY, VO-Y and $VO(opbmzl)_2$-Y are presented in Fig. 1. The XRD analysis showed that all peaks observed for the three materials can be assigned to the faujasite structure. VO-Y and $VO(opbmzl)_2$-Y complex exhibited identical diffraction patterns similar to that of NaY, except that the intensity of the peaks were considerably reduced and there was reversal in the peak intensities of (2 2 0), (3 1 1) and (3 3 1) planes. For instance, NaY and VO-Y showed the order; $I_{331} \gg I_{220} > I_{311}$, while it was $I_{331} \gg I_{311} > I_{220}$ for encapsulated complex. An empirical relationship subsists between the relative intensities of (3 3 1), (3 1 1) and (2 2 0) peaks and cation location in faujasite-type zeolite [20–22]. The variation in patterns further indicated that the VO^{+2} are substituted at the location of Na^+ could undergo rearrangement during complexation in the nanopores of zeolite-Y [23]. This observation may therefore be construed as an evidence for the successful encapsulation of $VO(opbmzl)_2$ complex within the supercage of zeolite-Y.

3.2 Spectroscopic characterization

FTIR spectra of ohpbmzl, NaY, $VO(opbmzl)_2$, $VO(opbmzl)_2Y$ and VO-Y were recorded as KBr disks (Fig. 2a–e). $VO(opbmzl)_2$ exhibited peaks at 3182, 1604 and 1313 cm^{-1} due to ν_{NH}, $\nu_{C=N}$ and ν_{C-N} respectively. A shift of the $\nu_{C=N}$ (ring) to lower frequency and absence of the ν_{OH} band in $VO(opbmzl)_2$ suggested the coordination of the tertiary nitrogen and phenolic oxygen of the ligand to VO^{2+}. $VO(opbmzl)_2Y$ exhibited peaks at 1381 and 1484 cm^{-1} due to ν_{C-N} and δ_{N-H} respectively. The $\nu_{V=O}$

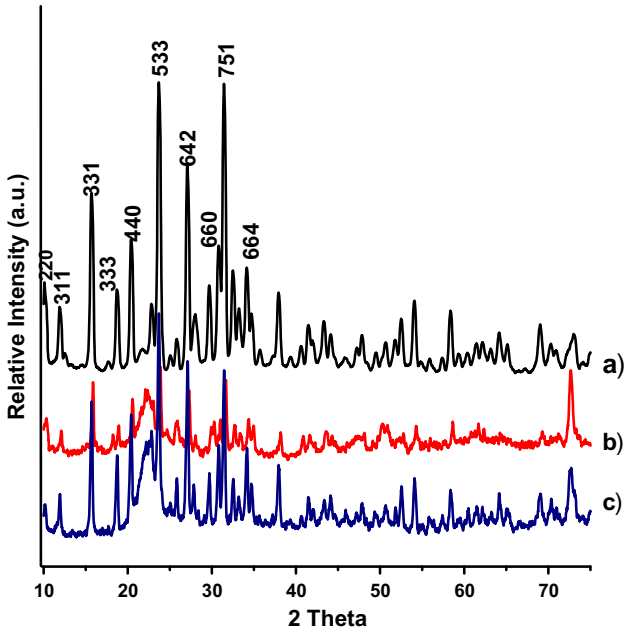

Fig. 1 Powdered XRD patterns of (**a**) NaY, (**b**) VO-Y and (**c**) $VO(opbmzl)_2Y$

peak was observed at 910 cm^{-1} for non-encapsulated complex and 906 cm^{-1} for $VO(opbmzl)_2$-Y. The peak due to sulphate group was absent in non-encapsulated and encapsulated complexes. Some of the peaks due to coordinated ligand were not observed in case of $VO(opbmzl)_2Y$, as they were obscured by zeolite peaks.

Electronic spectral data of ohpbmzl, VO-exchanged zeolite-Y (VO-Y), non-encapsulated and encapsulated $VO(opbmzl)_2$ complexes are shown in the Table 2. VO-Y exhibited bands at 613, 703 and 802 nm due to d–d transitions ascribed to octahedral coordination of vanadium(IV) in VO-Y. This further confirmed the successful exchange of Na^+ ions by VO^{2+}. $VO(opbmzl)_2$ exhibited intra-ligand bands at 204 ($\varphi \rightarrow \varphi^*$), 242 ($\pi \rightarrow \pi^*$) and 289 nm ($n \rightarrow \pi^*$) and LMCT band at 377 and three bands at 515, 751 and 786 nm due to d–d transition(s). The encapsulated $VO(opbmzl)_2$ complex showed intra-ligand transition bands at 213, 244 and 287 nm, band due to LMCT at 382 nm and d–d transition bands at 609, 669 and 728 nm which were attributed to $b_2 \rightarrow b_1$, $b_2 \rightarrow e$ and $b_2 \rightarrow a_1$ transitions respectively attesting a square pyramidal geometry of the vanadium(IV) complex in zeolite [24–26]. The intra-ligand transition and LMCT bands of zeolite encapsulated complex were red shifted with respect to $VO(opbmzl)_2$ owing to the influence of zeolite matrix on vanadium complex.

The room temperature ESR spectrum of VO-Y though not well resolved, was characteristic of VO^{2+} systems (V^{4+}, d^1) dominated by the axial hyperfine interaction between the unpaired electron spin (S = 1/2) and the ^{51}V nuclear spin (I = 7/2, 99.8 % natural abundance) (Fig. 3a). The $g_{\|}$ was found to be 1.917, while $g_{\perp}$ was 1.970 corresponding to the presence of $VO(H_2O)_5^{2+}$ [27]. The ESR spectrum of $V(opbmzl)_2Y$ showed a better resolved hyperfine splitting peaks as compared to VO-Y (Fig. 3b). The $g_{\|}$ was found to be 1.936 while $g_{\perp}$ was 1.984. $A_{\|}$ was found to be 147 G, while $A_{\perp}$ was 52 G. The g and A values are in agreement with the V center in square pyramidal geometry [28–30].

Based on FT-IR, electronic and ESR spectral data, a square pyramidal geometry was assigned to vanadium in $VO(opbmzl)_2Y$. In order for a complex to accommodate within the nano-cavity of zeolite-Y, its size should be less than the diameter of α-cage (~13 Å). The size of the vanadyl complex in the nano-cavity was found to be 11.12 Å (calculated using Guassview 5.0 software).

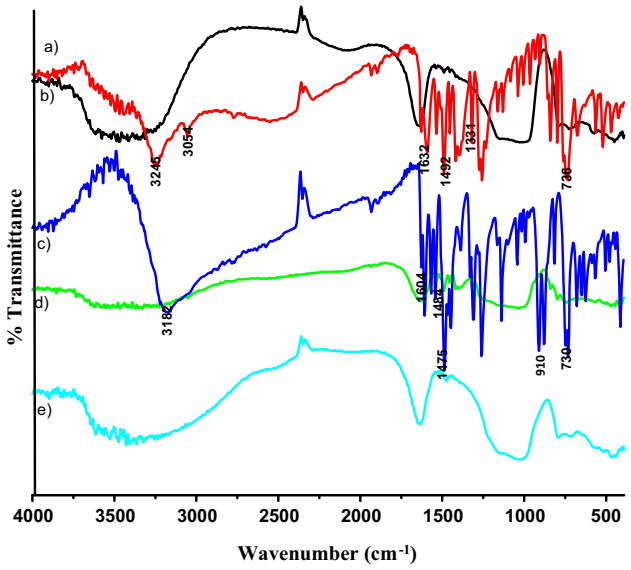

Fig. 2 IR spectra of (**a**) ohpbmzl; (**b**) NaY; (**c**) $VO(opbmzl)_2$; (**d**) $VO(opbmzl)_2$-Y and (**e**) VO-Y

3.3 Thermal analyses

VO-Y showed a single step decomposition profile pertaining to the loss of zeolitic water in the range of 100–250 °C (Fig. 4a). $VO(opbmzl)_2$ showed a sharp endothermic peak around 500 °C due to decomposition of complex with weight loss of ~47.0 %. The thermogram of the encapsulated complex displayed first decomposition at a temperature range of 60–200 °C which was due to loss of intra and extra framework water molecules (~11.1 %). The second decomposition in the range 200–330 °C could be due to the decomposition of complex which was ~3.9 %. Further weight loss was assigned to the decomposition of zeolite framework (Fig. 4b).

Table 2 Electronic spectral data (λ_{max} in nm) for the ligand, non-encapsulated and encapsulated complexes

Sample	φ → φ*	π → π*	n → π*	Charge transfer	d–d transitions
ohpbmzl	212	232, 250	264, 302	–	–
VO-Y	–	–	–	–	613, 703 and 802
$VO(opbmzl)_2$	204	242	289	377	578, 705 and 777
$VO(opbmzl)_2Y$	210	246	287	382	609, 708 and 784

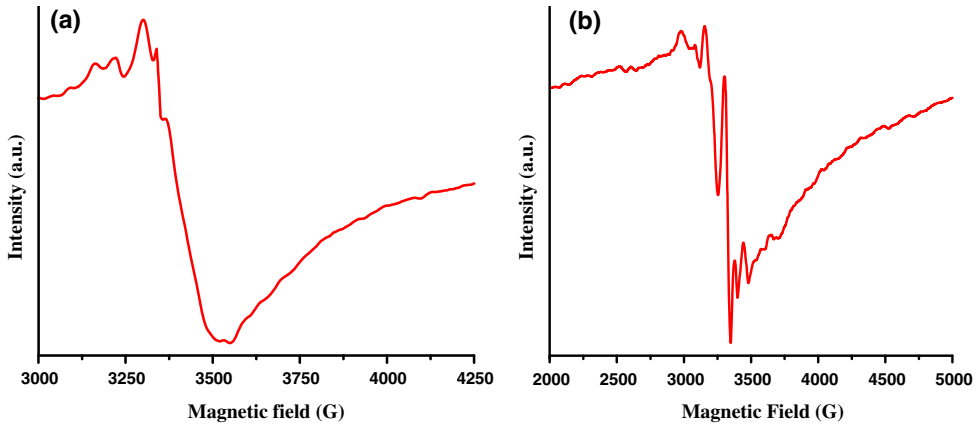

Fig. 3 **a** ESR spectra of VO-Y **b** $VO(opbmzl)_2Y$

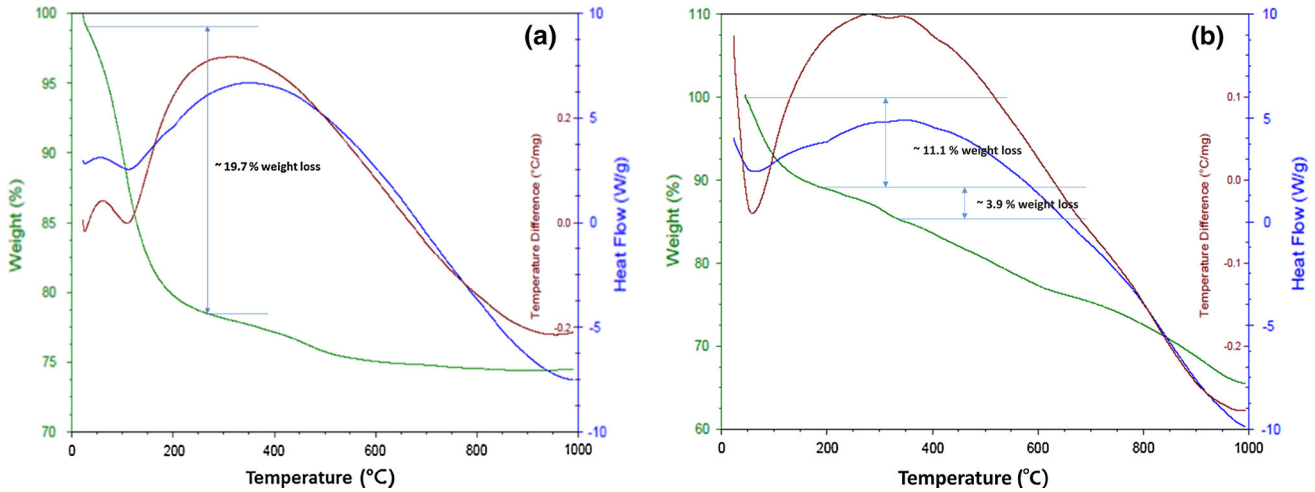

Fig. 4 **a** Thermograms of VO-Y; **b** $VO(opbmzl)_2$-Y

3.4 Electrochemical studies

Redox potential of metal is influenced by its immediate environment. It is observed that the redox potential of encapsulated complex varies greatly from that of the non-encapsulated complex. Hence, cyclic voltammetric studies were carried out to understand the electrochemical behavior of ligand, non-encapsulated and encapsulated complexes. The ligand exhibited a cathodic peak at −1.1358 V and an anodic peak at −0.9044 V due to one electron reduction [L → L̇] and oxidation [L̇ → L] respectively. The ligand redox peaks were observed for both non-encapsulated and encapsulated complexes. VO-Y exhibited two reduction peaks at −0.4715 and 0.2452 V due to V^V/V^{IV} and V^{IV}/V^{III} couple and two oxidation peaks at −0.3882 and 0.5749 V due to V^{III}/V^{IV} and V^{IV}/V^V couple respectively. The CV of non-encapsulated complex recorded in the solution mode displayed reduction potentials at −1.018 (ligand reduction), −0.5059 and 0.1047 V and oxidation potentials at −0.8777 (ligand oxidation), −0.4496 and 0.5051 V (Fig. 5a). The CV of non-encapsulated complex was also recorded in solid mode for comparison with the encapsulated complex. In solid mode, non-encapsulated complex exhibited a peak at −1.1023 (ligand reduction), −0.9055 (ligand oxidation), −0.646 V corresponding to an electrochemically quasi-reversible $V^V/$

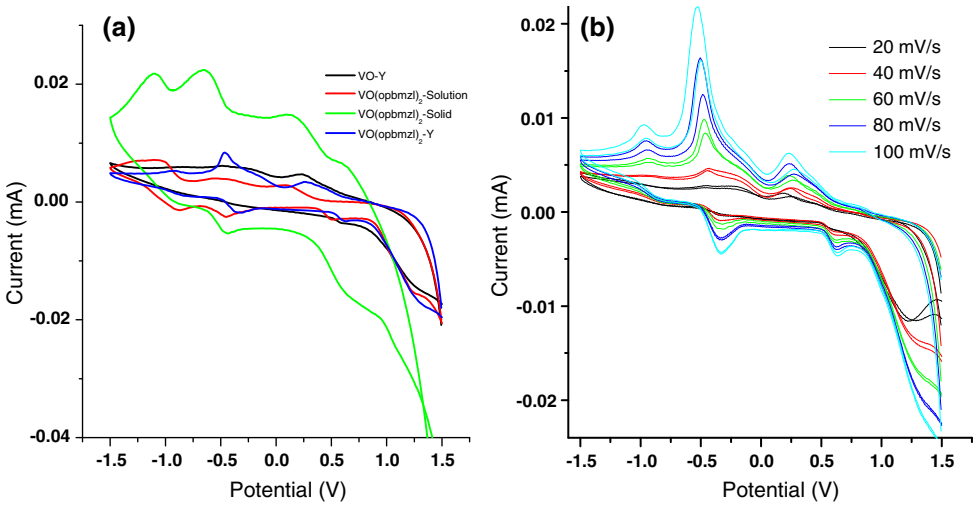

Fig. 5 Cyclic votammograms; **a** VO-Y, $VO(opbmzl)_2$ and $VO(opbmzl)_2$-Y **b** $VO(opbmzl)_2$-Y at different scan rates

Table 3 Influence of oxidant, temperature, substrate: oxidant ratio and concentration of catalyst on the phenol and styrene conversion

Phenol:Oxidant ratio	Oxidant	T (°C)	Catalyst (g)	V content (10^{-2} mmol)	Phenol conversion[a] (%)	Product selectivity (%)		
						CAT	HQ	BQ
1:1.5	TBHP	60	0.115	3.45	66.4	20.7	37.0	42.3
1:1.5	H_2O_2	60	0.115	3.45	64.8	47.8	32.7	19.5
1:1.0	H_2O_2	60	0.115	3.45	38.9	40.3	42.1	17.6
1:2	H_2O_2	60	0.115	3.45	66.7	32.6	36.8	30.6
1:1.5	H_2O_2	30	0.115	3.45	12.4	37.2	52.3	10.5
1:1.5	H_2O_2	40	0.115	3.45	26.1	40.7	47.1	12.2
1:1.5	H_2O_2	50	0.115	3.45	49.3	44.3	40.6	15.1
1:1.5	H_2O_2	70	0.115	3.45	66.8	32.3	30.2	37.5
1:1.5	H_2O_2	60	0.105	3.15	45.3	44.2	53.4	2.4
1:1.5	H_2O_2	60	0.125	3.75	55.7	29.2	62.2	8.7
Styrene:Oxidant ratio	Oxidant	T (°C)	Catalyst (g)	V content (10^{-2} mmol)	Styrene conversion[b] (%)	Product selectivity (%)		
						SO	BD	BA
1:2	TBHP	60	0.125	3.75	58.4	32.1	46.5	21.4
1:2	H_2O_2	60	0.125	3.75	53.1	42.3	38.9	18.8
1:1	H_2O_2	60	0.125	3.75	42.3	40.2	40.5	19.3
1:3	H_2O_2	60	0.125	3.75	55.9	29.3	40.6	30.1
1:2	H_2O_2	30	0.125	3.75	8.3	29.7	58.0	12.3
1:2	H_2O_2	40	0.125	3.75	26.7	30.2	45.5	24.3
1:2	H_2O_2	50	0.125	3.75	34.8	31.9	45.5	22.6
1:2	H_2O_2	70	0.125	3.75	55.7	29.2	28.5	42.3
1:2	H_2O_2	60	0.115	3.45	26.7	29.4	69.1	1.5
1:2	H_2O_2	60	0.135	4.05	41.3	27.6	56.0	16.4

Reaction conditions: [a] Solvent: CH_3CN, 6 mL; [phenol] = 50 mol; *T* temperature, *CAT* catechol, *HQ* hydroquinone, *BQ* benzoquinone. [b] Solvent: CH_3CN, 10 mL; [styrene] = 50 mol; *SO* styrene oxide, *BD* benzaldehyde, *BA* benzoic acid

V^{IV} transition, whereas 0.1543 V features a reduction of V^{IV} to the corresponding V^{III} complex (Fig. 5a). The peaks at −0.4496 and 0.6945 V correspond to the V^{III}/V^{IV} and V^{IV}/V^{V} couple, respectively. The $VO(opbmzl)_2$-Y complex displayed cathodic peaks at −0.4639 and 0.2729 V due to V^{IV}/V^{III} and V^{V}/V^{IV} respectively (Fig. 5b). Two anodic

peaks at −0.3377 and 0.6102 V were assigned to V^{IV}/V^{V} and V^{III}/V^{IV} respectively. It also exhibited peaks at −0.9196 and −0.8003 V due to reduction and oxidation of ligand respectively. These redox potential values were completely different from that of the VO-exchanged zeolite-Y and $VO(opbmzl)_2$ both in solid and solution mode, which substantiated the formation of complex inside zeolite-Y. Compared to non-encapsulated complex, the peaks were relatively broadened and average reduction potential values were shifted to more positive values upon encapsulation which was mainly attributed to the interaction of metal complex with the walls of the zeolite matrix. During the course of interaction, metal complex may perturb all the active sites present within the zeolite, inducing different interaction energies and alter redox potential at different places in the zeolite [31]. The alteration of peak potential indicated that the metal complex is encapsulated inside the zeolite matrix and not present on the external surface. If there is any drastic decrease in peak currents for zeolite modified electrode, then the electron transfer occurs via extra-zeolite mechanism [32–34]. It was observed that CV of the encapsulated complex showed no decrease in peak currents, found to be independent of scan rate and was stable over an extended period of time without any change in redox potential values (Fig. 5b), which was indicative of intrazeolite mechanism.

4 Oxidation studies

To determine suitable reaction conditions for maximum conversion of substrates, the effects of oxidant, temperature, catalyst amount and substrate: H_2O_2 ratio were investigated using [$VO(opbmzl)_2$]-Y catalyst for oxidation of phenol, styrene, cyclohexane and ethyl benzene. The blank test for phenol, styrene, cyclohexane and ethyl benzene using H_2O_2 under other optimized conditions were carried out, which showed 17.4, 9.5, 1.9 and 10.9 % conversion respectively.

4.1 Oxidation of phenol

The oxidation of phenol catalyzed by $VO(opbmzl)_2$-Y using H_2O_2 as oxidant gave catechol and hydroquinone as major products and benzoquinone as a minor product. Phenol conversion was 64.8 % with selectivity towards catechol, hydroquinone and benzoquinone was 47.8, 32.7 and 19.5 % respectively.

The reaction was carried out using two different oxidants viz. H_2O_2 and TBHP using 50 mol of phenol, 0.115 g of catalyst, 75 mol of oxidant in 6 ml CH_3CN at 60 °C for 6 h. The conversion of phenol with TBHP was 66.4 % with 20.7, 37.0 and 42.3 % selectivity towards catechol, hydroquinone and benzoquinone respectively, while phenol conversion was 64.8 % with 47.8, 32.7 and 19.5 % selectivity towards catechol, hydroquinone and benzoquinone with H_2O_2. Though the phenol conversion was slightly higher in TBHP, catechol selectivity was low as compared to H_2O_2 (Table 3). Hence, H_2O_2 was used as an oxidant for phenol oxidation. In order to determine the effect of phenol/H_2O_2 molar ratio on phenol oxidation, three different molar ratios (1:1, 1:1.5 and 1:2) were studied, whilst keeping a fixed amount of phenol (50 mmol) and $VO(opbmzl)_2$-Y (0.115 g) in 6 ml of CH_3CN at 60 °C and running the reaction for 6 h (Fig. 5). It was observed that in 1:1 molar ratio, phenol conversion was 38.9 % with 40.3, 42.1 and 17.6 % selectivity towards catechol, hydroquinone and benzoquinone respectively. When the ratio was increased to 1:1.5, phenol conversion increased to 64.8 % with 47.8, 32.7 and 19.5 % selectivity towards catechol, hydroquinone and benzoquinone. Further increase in molar ratio to 1:2, lead to slight increase in phenol conversion (66.7 %) but catechol and hydroquinone selectivity decreased (32.6 and 36.8 % respectively) (Table 3).

The effect of temperature on the oxidation of phenol was investigated at 30, 40, 50, 60 and 70 °C whilst keeping all the other parameters constant over a period of 6 h (Table 3). The percentage conversion and catechol selectivity increased gradually with increase in temperature from 30 to 70 °C. The order of phenol conversion was found to be; 70 °C (66.8 %) > 60 °C (64.8 %) > 50 °C (49.3 %) > 40 °C (26.1 %) > 30 °C (12.4 %) whereas catechol selectivity was in the order; 60 °C (47.8 %) > 50 °C (44.3 %) > 40 °C (40.7 %) > 30 °C (37.2 %) > 70 °C (32.3 %).

The effect of catalyst concentration on phenol conversion was investigated using 0.105, 0.115 and 0.125 g (Table 4). When 0.105 g of catalyst was used, conversion of phenol and catechol selectivity was found to be 45.3 and 44.2 % respectively. With further increase to 0.115 g, conversion increased to 64.8 % with slight increase in catechol selectivity (47.8 %). However, with 0.125 g of catalyst, percentage conversion and selectivity towards catechol decreased to 55.7 and 29.2 % respectively.

The catalytic activity of $VO(opbmzl)_2$Y was compared with NaY, VO-Y and $VO(opbmzl)_2$ towards phenol oxidation using 1.9 g of phenol (50 mmol) with 30 % H_2O_2 (8.5 g; 75 mmol) in 6 mL CH_3CN at 60 °C for 6 h. The percentage phenol conversion for these catalysts was found to be in the order; $VO(opbmzl)_2$-Y (64.8 %) > $VO(opbmzl)_2$ (54.1 %) > VO-Y (53.6 %) > NaY (22.6 %), whereas the selectivity towards catechol was found to be in the order; $VO(opbmzl)_2$-Y (47.8 %) > VO-Y (43.9 %) > $VO(opbmzl)_2$ (40.4 %) > NaY (18.6 %) (Fig. 6). Though the percentage conversion of phenol was

Table 4 Influence of oxidant, temperature, substrate: oxidant ratio and concentration of catalyst on the cyclohexane and ethyl benzene conversion

Cyclohexane:Oxidant ratio	Oxidant	T (°C)	Catalyst (g)	V content (10^{-2} mmol)	Cyclohexane[c] conversion (%)	Product selectivity (%)	
						OL	ONE
1: 2	TBHP	60	0.135	4.05	50.9	49.7	50.3
1: 2	H_2O_2	60	0.135	4.05	48.3	48.5	51.5
1: 1	H_2O_2	60	0.135	4.05	10.6	54.3	45.7
1: 3	H_2O_2	60	0.135	4.05	16.6	39.9	60.1
1.2	H_2O_2	30	0.135	4.05	22.5	75.5	24.5
1:2	H_2O_2	40	0.135	4.05	32.5	70.3	29.7
1:2	H_2O_2	50	0.135	4.05	37.9	64.2	35.8
1:2	H_2O_2	70	0.135	4.05	46.2	48.0	52.0
1: 2	H_2O_2	60	0.125	3.75	35.2	55.3	44.7
1: 2	H_2O_2	60	0.145	4.35	39.7	50.4	49.6

EB:Oxidant ratio	Oxidant	T (°C)	Catalyst(g)	V content (10^{-2} mmol)	EB[d] conversion (%)	Product selectivity (%)		
						AP	BD	BA
1:2	TBHP	60	0.125	3.75	59.4	44.6	53.3	2.1
1:2	H_2O_2	60	0.125	3.75	57.9	61.9	37.0	1.1
1:1	H_2O_2	60	0.125	3.75	41.3	39.5	59.0	1.5
1:3	H_2O_2	60	0.125	3.75	58.1	34.2	61.3	4.5
1:2	H_2O_2	30	0.125	3.75	11.9	29.4	70.5	0.05
1:2	H_2O_2	40	0.125	3.75	21.6	32.9	67.0	0.08
1:2	H_2O_2	50	0.125	3.75	36.9	41.7	58.2	0.12
1:2	H_2O_2	70	0.125	3.75	58.2	54.3	37.8	7.9
1:2	H_2O_2	60	0.115	3.45	32.6	46.3	53.7	0.05
1:2	H_2O_2	60	0.135	4.05	52.3	37.2	62.5	0.3

Reaction conditions: [c] Solvent: CH_3CN, 10 mL; [cyclohexane]: 50 mol; *OL* cyclohexanol, *ONE* cyclohexanone; [d] Solvent: CH_3CN, 6 mL; [ethylbenzene]: 50 mol; *AP* acetophenone, *EB* ethyl benzene

almost same in non-encapsulated complex and VO-Y, the selectivity towards catechol was found to be higher in case of encapsulated complex and VO-Y.

4.2 Oxidation of styrene

In a typical reaction, styrene (5.2 g; 50 mmol) and 30 % H_2O_2 (3.4 g; 100 mmol) in 10 mL CH_3CN was heated with continuous stirring at 70 °C for 6 h using 0.125 g of $VO(opbmzl)_2$-Y which gave styrene conversion of 53.1 % with 42.3, 38.9 and 18.8 % selectivity towards styrene oxide, benzaldehyde and benzoic acid respectively. The reaction was also studied using TBHP as oxidant by keeping other parameters constant. With TBHP, 58.4 % styrene conversion was observed with 32.1, 46.5 and 21.4 % selectivity towards styrene oxide, benzaldehyde and benzoic acid respectively (Table 3). Since selectivity towards styrene oxide was higher with H_2O_2 (42.3 %), it was selected as oxidant to carry out further reactions.

Similarly, reaction was carried out for three different styrene/H_2O_2 molar ratios viz. 1:1, 1:2 and 1:3, keeping other parameters constant. Percentage styrene conversion was found to be in the order 1:3 (55.9 %) > 1:2 (53.1 %) > 1:1 (42.3 %), whereas selectivity towards styrene oxide was found to be in the order: 1:2 (42.3 %) > 1:1 (40.2 %) > 1:3 (29.3 %). Even though styrene conversion was slightly higher using 1:3 molar ratio, selectivity towards styrene oxide decreased. With increase in temperature from 30 to 70 °C, styrene conversion increased from 8.3 to 55.7 %, while the selectivity towards styrene oxide gradually increased from 29.7 (at 30 °C) to 42.3 % at 60 °C but it decreased to 29.2 % at 70 °C. Moreover, at this temperature, selectivity towards benzoic acid was more prominent (42.3 %) (Table 3).

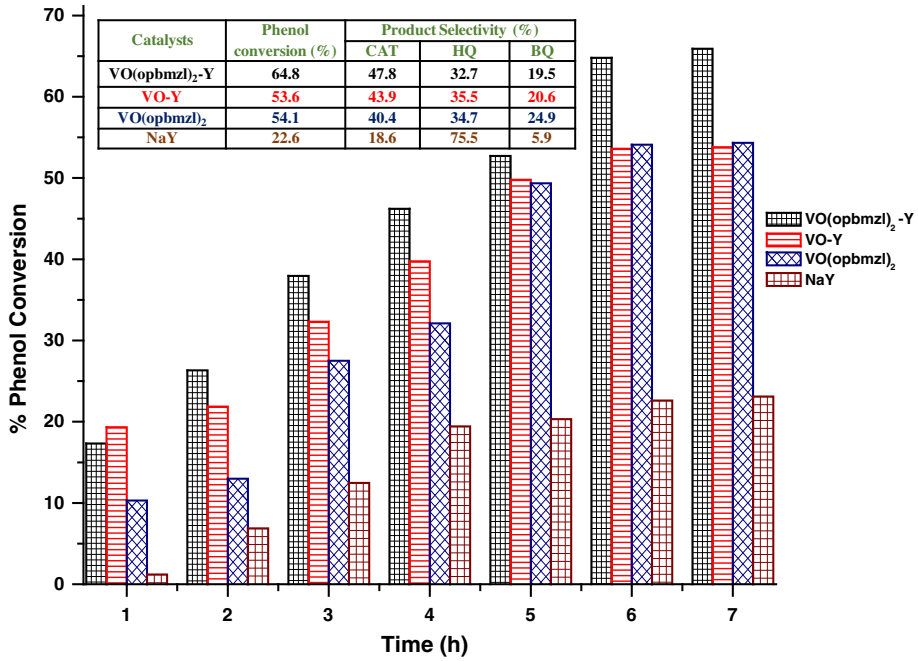

Fig. 6 Effect of catalysts on % phenol conversion and product selectivity

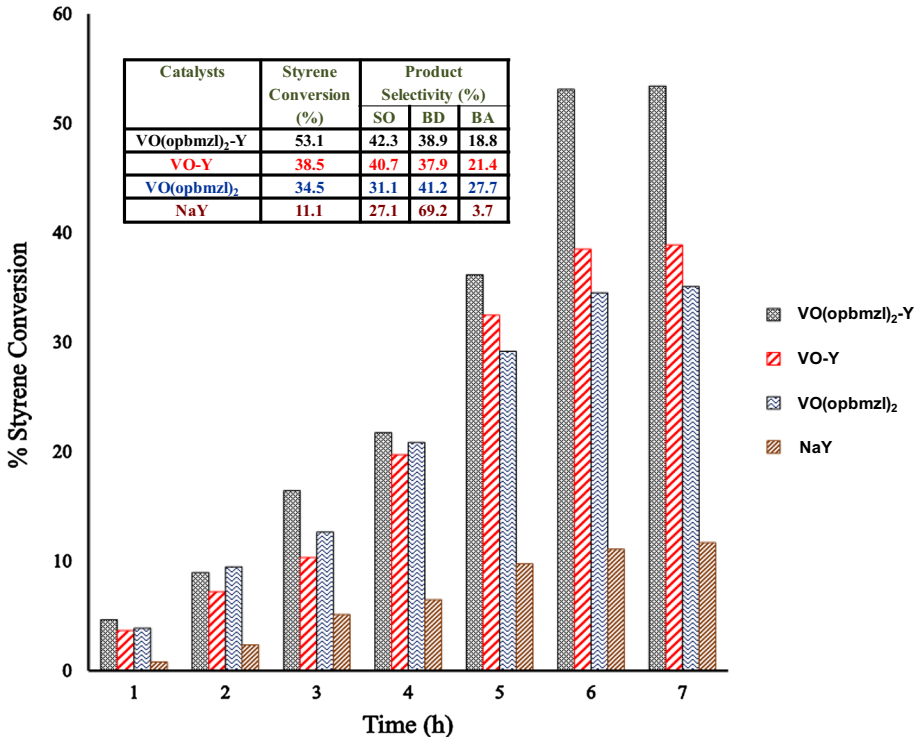

Fig. 7 Effect of catalysts on % styrene conversion and product selectivity

With variation of different amounts of catalyst (0.115, 0.125 and 0.135 g), 0.125 g showed better conversion (53.1 %) and selectivity towards styrene oxide (42.3 %) whereas at lower concentration of catalyst (0.115 g), styrene conversion was found to be 26.7 with 29.4 % selectivity towards styrene oxide (Table 3). Increase in concentration to 0.135 g, decreased the conversion to 41.3 with 21.6 % selectivity towards styrene oxide.

Figure 7 shows the profiles for conversion of styrene using NaY, VO-Y, $VO(opbmzl)_2$ and $VO(opbmzl)_2$-Y as catalysts. It indicated that the performance of the encapsulated catalyst was higher than that of non-encapsulated analogue. The percentage styrene conversion and styrene oxide selectivity was found to be in the order; $VO(opbmzl)_2$-Y (53.1, 42.3 %) > VO-Y (38.5, 40.7 %) > $VO(opbmzl)_2$ (34.5, 31.1 %) > NaY (11.1, 27.1 %).

Catalysts	Cyclohexane Conversion (%)	Product Selectivity (%)	
		OL	ONE
$VO(opbmzl)_2$-Y	48.3	48.5	51.5
VO-Y	12.7	62.3	37.7
$VO(opbmzl)_2$	24.3	58.1	41.9
NaY	2.2	82.9	17.1

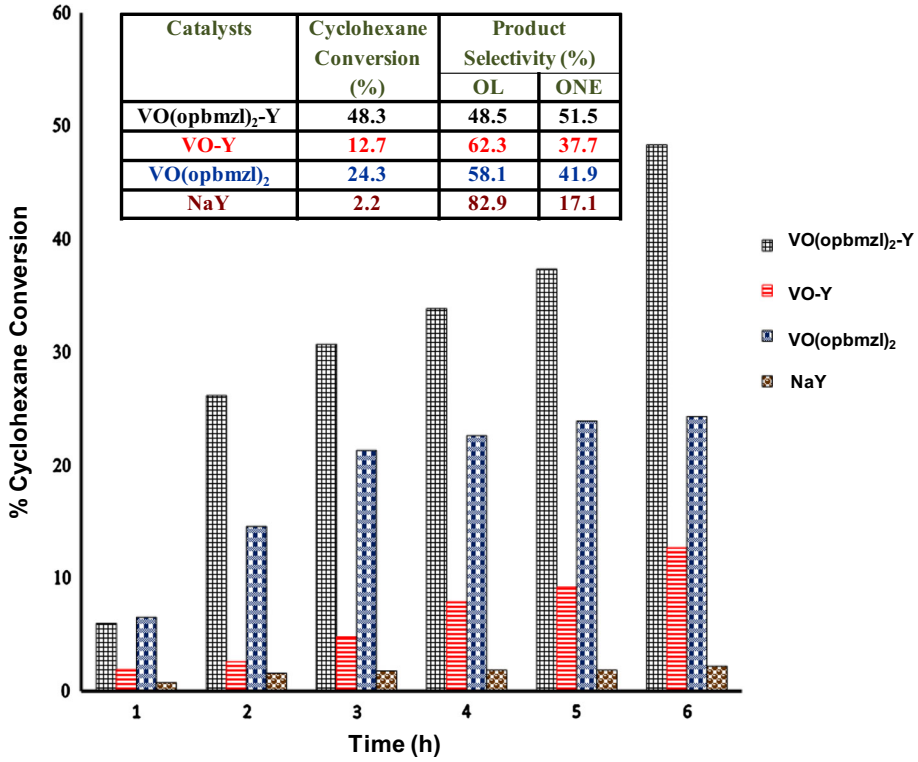

Fig. 8 Effect of catalysts on % cyclohexane conversion and product selectivity

Catalysts	Ethyl benzene Conversion (%)	Product Selectivity (%)		
		AP	BD	BA
$VO(opbmzl)_2$-Y	57.9	61.9	37.0	1.1
VO-Y	43.5	39.5	57.2	3.3
$VO(opbmzl)_2$	40.6	27.8	64.3	7.9
NaY	27.4	54.9	38.3	6.8

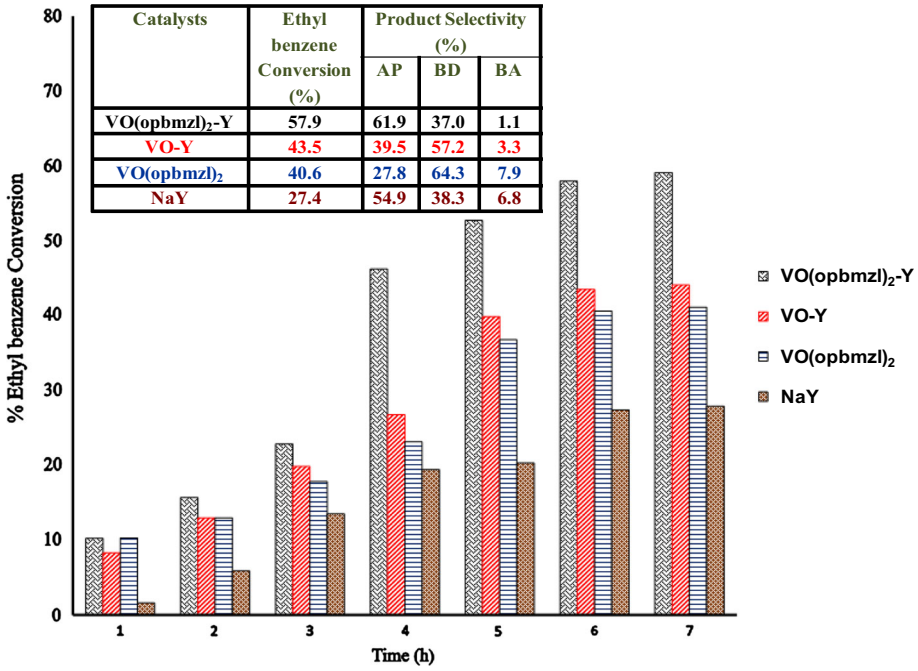

Fig. 9 Effect of catalysts on % ethylbenzene conversion and product selectivity

4.3 Oxidation of cyclohexane

Effect of oxidant on cyclohexane conversion was investigated using 75 mmol of cyclohexane, 0.135 g of catalyst, 150 mmol of oxidant in 10 mL CH_3CN at 60 °C for 6 h. TBHP gave 50.9 % cyclohexane conversion with 49.7 and 50.3 % selectivity towards cyclohexanol and cyclohexanone, while H_2O_2 gave 48.3 % cyclohexane conversion with 48.5 and 51.5 % selectivity towards cyclohexanol and cyclohexanone (Table 4). Though TBHP gave slightly higher conversion (~2.6 %), selectivity towards cyclohexanol and cyclohexanone almost remained same. Hence H_2O_2 was chosen as oxidant for cyclohexane oxidation.

Table 5 Recycling studies of the catalyst

Catalytic runs	% Phenol conversion[a]	Selectivity of products (%)		
		CAT	HQ	BQ
I	64.8	47.8	32.7	19.5
II	64.0	47.5	32.3	20.2
III	60.9	46.1	29.4	24.5
IV	53.7	41.3	23.8	34.9
V	44.1	35.6	17.9	46.5
Catalytic runs	% Styrene conversion[b]	Selectivity of products (%)		
		SO	BD	BA
I	53.1	42.3	38.9	18.8
II	52.8	42	37.1	20.9
III	50.7	39.9	34.3	25.8
IV	47.2	36.4	30.1	33.5
V	41.4	32.5	23.1	44.4
Catalytic runs	% Cyclohexane conversion[c]	Selectivity of products (%)		
		OL	ONE	
I	48.3	48.5	51.5	
II	44.9	49.1	50.9	
III	41.3	49.3	50.7	
IV	37.2	50.9	49.1	
V	31.5	54.4	45.6	
Catalytic runs	% Ethyl benzene conversion[d]	Selectivity of products (%)		
		AP	BD	BA
I	57.9	61.9	37	1.1
II	57.1	60.4	36.2	3.4
III	53.2	58.2	35.5	6.3
IV	48.1	54.6	31.2	14.2
V	42.6	48.1	25.6	26.3

Reaction conditions: [a] Solvent: CH_3CN, 6 mL; $[VO(opbmzl)_2\text{-}Y] = 0.115$ g; [phenol] = 50 mol; $[H_2O_2] = 75$ mol, temperature 60 °C. [b] Solvent CH_3CN, 10 mL; $[VO(opbmzl)_2\text{-}Y] = 0.125$ g; [styrene] = 50 mol; $[H_2O_2] = 100$ mol; temperature 70 °C. [c] Solvent: CH_3CN, 10 mL; $[VO(opbmzl)_2\text{-}Y] = 0.135$ g; [cyclohexane] = 75 mol; $[H_2O_2] = 150$ mol; temperature 60 °C. [d] Solvent CH_3CN, 6 mL; $[VO(opbmzl)_2\text{-}Y] = 0.115$ g; [ethyl benzene] = 50 mol; $[H_2O_2] = 100$ mol; temperature 60 °C

In order to determine the effect of cyclohexane/H_2O_2 molar ratio, the reaction was carried out with three different molar ratios (1:1, 1:2 and 1:3), whilst keeping a fixed amount of cyclohexane (75 mmol) and $VO(opbmzl)_2$-Y (0.135 g) in 10 ml of CH_3CN at 60 °C and running the reaction for 6 h (Table 4). At 1:1 molar ratio, the conversion was only 10.6 % with 54.3 and 45.7 % selectivity towards cyclohexanol and cyclohexanone respectively. When the ratio was increased to 1:2, conversion increased to 48.3 with 48.5 % cyclohexanol and 51.5 % cyclohexanone selectivity. With further increase in the ratio to 1:3, conversion of cyclohexane drastically decreased to 16.6 % with 39.9 % cyclohexanol selectivity and 60.1 % cyclohexanone. This may be due to increase in cyclohexane: H_2O_2 ratio would increase dilution of reaction mixture (due to presence of water in 30 % H_2O_2), thus leading to decreased % conversion of cyclohexane. Hence, 1:2 molar ratio was considered as optimum for cyclohexane oxidation using $VO(opbmzl)_2$-Y. The performance of $VO(opbmzl)_2$-Y towards cyclohexane oxidation was investigated at five different temperatures, viz. 30, 40, 50, 60 and 70 °C whilst keeping all the other parameters constant over a period of 6 h (Table 4). At 30 °C, the reaction showed a low conversion (22.5 %) but high selectivity for cyclohexanol formation (75.5 %). On increasing the temperature to 60 °C, conversion increased to 48.3 %, with 51.5 and 48.5 % selectivity towards cyclohexanol and cyclohexanone respectively. Further, by increasing the temperature to 70 °C no appreciable increase in cyclohexane conversion (46.2 %) or in cyclohexanone selectivity (52.0 %) was observed. Hence, 60 °C was optimized for the reaction.

Cyclohexane oxidation was carried out with three different amounts of catalysts (0.125, 0.135, 0.145 g) whilst keeping the other parameters constant. The results indicated that increasing the concentration of catalyst from 0.125 to 0.135 g increased the conversion from 35.2 to 48.3 % at 6 h (Table 4). Further increase in catalyst amount to 0.145 g resulted in decreasing the percentage conversion to 39.7 with 49.6 % selectivity towards cyclohexanone.

Under optimized reaction conditions, i.e. 75 mmol of cyclohexane, cyclohexane/H_2O_2 molar ratio of 1:2, with 0.135 g of catalyst in 10 mL CH_3CN and at 60 °C, Na-Y, VO-Y, $VO(opbmzl)_2$-Y complex and non-encapsulated $VO(opbmzl)_2$ were tested for cyclohexane oxidation and the results are illustrated in Fig. 8. It was observed that $VO(opbmzl)_2$-Y showed higher selectivity towards cyclohexanone whereas other catalysts exhibited higher selectivity towards cyclohexanol. At 60 °C and 6 h reaction time, the cyclohexane conversion and selectivity towards cyclohexanone followed the order; $VO(opbmzl)_2$-Y (48.3, 51.5 %) > $VO(opbmzl)_2$ (24.3, 41.9 %) > VO-Y (12.7, 37.7 %) > NaY (2.2, 17.1 %). The enhanced activity of zeolite-encapsulated complex in the cyclohexane oxidation may be due to the interaction of metal complex with the zeolite framework and easy access of the active sites to cyclohexane.

4.4 Oxidation of ethylbenzene

Oxidation of ethylbenzene by using $VO(opbmzl)_2$-Y yields acetophenone and benzaldehyde as major products, with

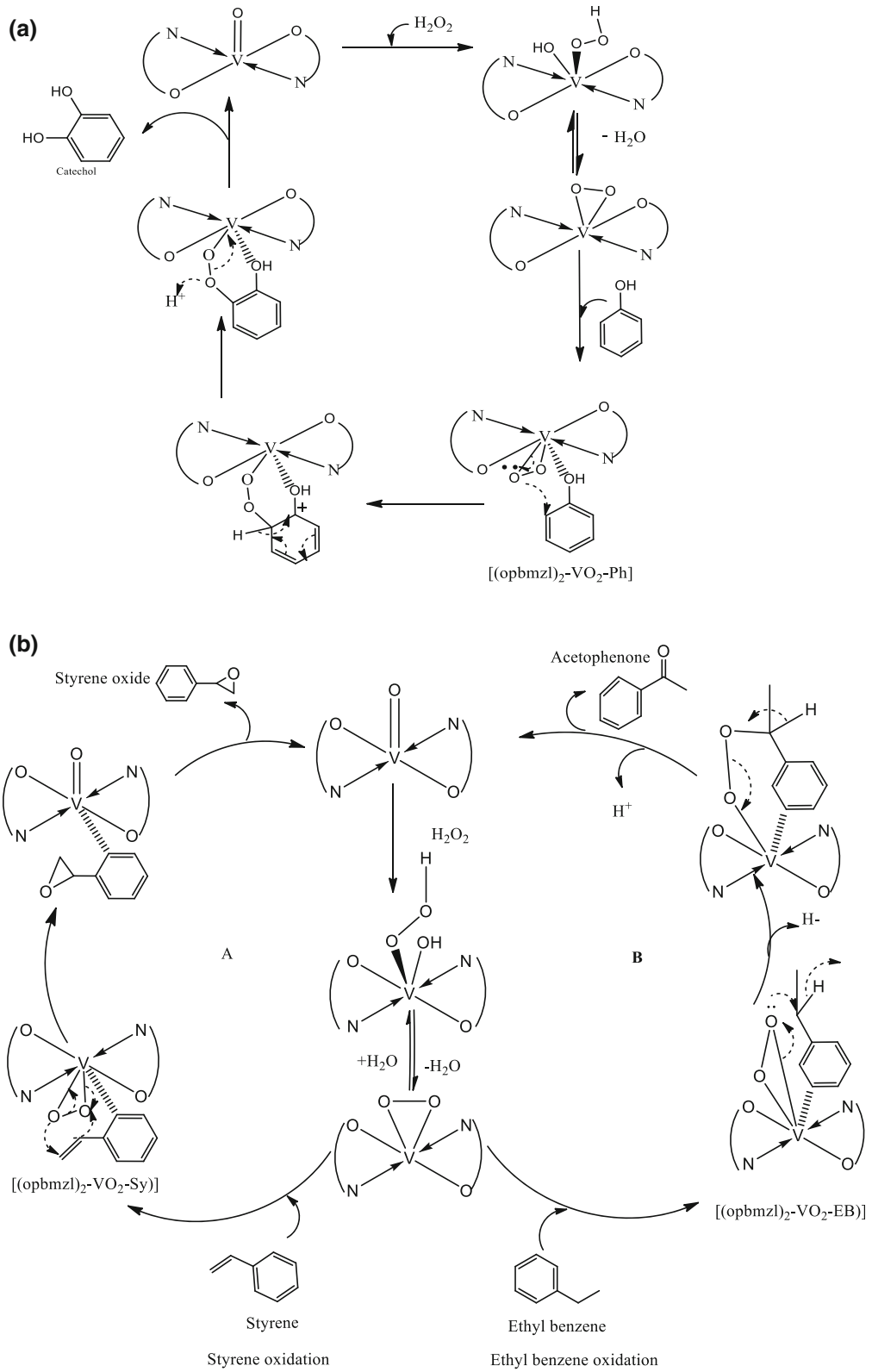

Scheme 2 **a** Mechanism of phenol oxidation using VO(opbmzl)$_2$-Y, **b** Mechanism of [A] styrene and [B] ethyl benzene oxidation using VO(opbmzl)$_2$-Y, **c** Mechanism of cyclohexane oxidation using VO(opbmzl)$_2$-Y

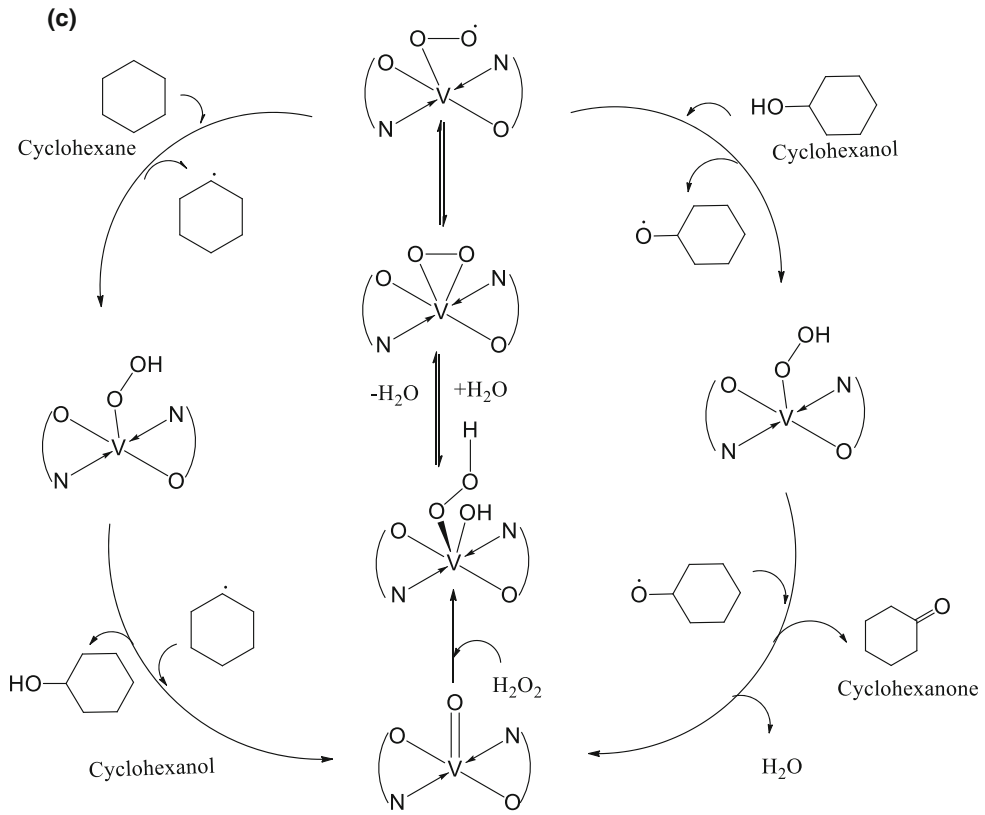

Scheme 2 continued

benzoic acid in minor yield. In a typical reaction, 50 mol of ethyl benzene and 100 mol of 30 % H_2O_2 in 10 mL CH_3CN at 60 °C for 6 h using 0.125 g of catalyst to yield acetophenone and benzaldehyde (61.9 and 37.0 % selectivity) and benzoic acid (1.1 % selectivity).

The effect of H_2O_2 and TBHP as oxidants was studied using 50 mol of ethylbenzene, 0.125 g of catalyst, 100 mol of oxidant in 6 ml CH_3CN at 60 °C for 6 h. TBHP gave 59.4 % ethylbenzene conversion with 44.6 and 53.3 and 2.1 % selectivity towards acetophenone, benzaldehyde and benzoic acid respectively. Using H_2O_2, ethyl benzene conversion was 57.9 % with 61.9 and 37.0 % selectivity towards acetophenone and benzaldehyde (Table 4). Similarly, the reaction was carried out using three different ethylbenzene: H_2O_2 molar ratio viz. 1:1, 1:2 and 1:3 under optimized conditions (Table 4). The ethylbenzene conversion increased from 41.3 to 58.1 % with increase in ratio from 1:1 to 1:3. However, selectivity to acetophenone followed the order: 1:2 (61.9 %) > 1:1 (39.5 %) > 1:3 (34.2 %). Moreover, increase in molar ratio to 1:3, enhanced the formation of benzoic acid (4.5 %). Hence, 1:2 molar ratio was optimized for ethylbenzene oxidation. At lower molar ratio (1:1), % conversion decreased, which may be due to insufficient amount of oxidant for conversion of substrates.

The reaction was carried out by varying the temperatures in the range 30–70 °C keeping all other parameters constant (Table 4). Ethylbenzene conversion increased from 11.9 % at 30 °C to 58.2 % at 70 °C, but the selectivity towards acetophenone increased from 29.4 % (30 °C) to 61.9 % at 60 °C. Further increase in temperature to 70 °C, resulted in the formation of benzoic acid with decrease in selectivity towards acetophenone (54.3 %). Hence, 60 °C was optimized for ethylbenzene oxidation. Increase in % conversion at higher temperature may be due to further decrease in activation energy of the reaction.

Reaction was carried out using three different catalyst concentration; viz., 0.115 g, 0.125 g and 0.135 g maintaining other conditions constant, % conversion was found to be in the order; 0.125 g (57.9 %) > 0.135 g (52.3 %) > 0.115 g (32.6 %), while selectivity towards acetophenone followed the order; 0.125 g (61.9 %) > 0.115 g (46.3 %) > 0.135 g (37.2 %) (Table 4). Decrease in activity at a higher amount of catalyst (0.145 g) might possibly be due to chemisorption of the reactant and oxidant molecules on

different active sites, thereby reducing the possibility to interact. The % conversion of ethylbenzene among the catalysts was found to be in the order; $VO(opbmzl)_2$-Y (57.9 %) > VO-Y (43.5 %) > $VO(opbmzl)_2$ (40.6 %) > NaY (27.4 %), while the acetophenone selectivity was found to be; $VO(opbmzl)_2$-Y (61.9 %) > NaY (54.9 %) > VO-Y (39.5 %) > $VO(opbmzl)_2$ (27.8 %) (Fig. 9). Higher activity of encapsulated complex as compared to the non-encapsulated homologue showed that the zeolite framework has a remarkable influence on catalytic activity and selectivity towards the product, may be attributed to the volume constraint and electronic effects of the matrix on the active species inside the framework.

5 Recycling ability and leaching test

The recycling ability of the $VO(opbmzl)_2Y$ was investigated by separating the catalyst from the reaction mixture after the reactions. It was then washed with CH_3CN, dried at 120 °C and reused for oxidation reactions under optimized conditions. The results showed that catalyst was almost stable up to three runs with decrease in substrate conversion thereafter (Table 5). Thus, the encapsulation of complex in zeolite was found to increase the life of the complex inside the zeolite cavity and the zeolite framework keeps the metal complexes dispersed by reducing dimerization due to restriction of internal framework structure leading to the retention of catalytic activity. To test the heterogeneous nature of the reactions in presence of $VO(opbmzl)_2Y$, reactions were carried out under optimized conditions for 3 h. Later the catalyst was removed from the reaction mixture and the reaction was further carried out for 3 more hours. It was observed that there was no increased conversion of substrates in absence of catalyst. The solution was tested for any vanadium content by AAS. The absence of vanadium in solution indicated that the metal has not leached out from the catalyst and it was heterogeneous in nature.

6 Mechanism

To check whether the reactions proceeded via free radical mechanism or not, all the reactions were carried out using non-encapsulated and encapsulated catalyst in presence of BHT, which is a hydroxyl free radical scavenger. Since, oxidation of phenol, styrene and ethylbenzene proceeded even in presence of BHT, it was confirmed that the reactions did not occur via free radical mechanism whereas cyclohexane oxidation did not proceed, which indicated that it followed free radical mechanism.

Vanadyl complexes are known to catalyze oxidation of organic substrates via formation of oxoperoxovanadium (V) intermediates [35]. These intermediates later attack the substrate and carry out oxidation by transfer of oxygen. The interaction of H_2O_2 with $VO(opbmzl)_2$ (both free and encapsulated) produced active oxoperoxovanadium (V) intermediate species [$(opbmzl)_2$-VO_2]. The non-encapsulated and encapsulated $VO(opbmzl)_2$ complexes produced an active species [$(opbmzl)_2$-VO_2-Ph], [$(opbmzl)_2$-VO_2-Sy] and [$(opbmzl)_2$-VO_2-EB] in case phenol hydroxylation, styrene epoxidation and ethylbenzene oxidation respectively.

In case of phenol oxidation, the intermediate [$(opbmzl)_2$-VO_2-Ph] underwent rearrangement to produce catechol and hydroquinone (Scheme 2a). The interactions in intermediate [$(opbmzl)_2$-VO_2-Sy] was assisted with the transfer of oxygen to produce styrene oxide and other reaction products in the epoxidation of styrene (Scheme 2b [A]). Benzaldehyde may be produced by further interaction of styrene oxide with the intermediate [$(opbmzl)_2$-VO_2-Sy] causing C–C bond cleavage. In case of ethylbenzene, non-radical mechanism via the formation of intermediate [$(opbmzl)_2$-VO_2-EB] which further underwent nucleophilic attack of coordinated peroxo oxygen to the benzylic carbon forming acetophenone (Scheme 2b [B]).

The oxidation of cyclohexane by oxovanadium complex is known to occur via free radical mechanism through the formation of cyclohexyloxy ($C_6H_{11}O\cdot$) and cyclohexyl ($C_6H_{11}\cdot$) radicals which further react to form cyclohexanol and cyclohexanone (Scheme 2c).

7 Conclusion

$VO(opbmzl)_2$ has been encapsulated in the supercage of zeolite-Y. Chemical analysis revealed the presence of low concentration of metal complex in the supercages of zeolite. The reduction of surface area and pore volume supported the fact that the complexes were within the cavities of zeolite. The XRD analysis suggested that the crystallinity of the zeolite was preserved during encapsulation. UV–Vis and ESR spectral data indicated a square pyramidal coordination of vanadium in the encapsulated complex. Redox potentials of encapsulated complex were found to be different from that of non-encapsulated complex and VO-Y, attesting the successful encapsulation of the complex within the framework. The encapsulated complex catalyzed the oxidation of phenol, styrene, cyclohexane and ethylbenzene with high conversion and selectivity as compared to non-encapsulated complex and was stable up to three runs.

Acknowledgments Authors thank Department of Chemistry, Bangalore University for providing instrumentation facilities and Prof. P. V. Kamath for cyclic voltammetric instrumentation.

References

1. S.J.J. Titinchi, G.V. Willingh, H.S. Abbo, R. Prasad, Catal. Sci. Technol. **5**, 325–338 (2015)
2. K.K. Bania, R.C. Deka, J. Phys. Chem. C **117**(22), 11663–11678 (2013)
3. C.K. Modi, B.G. Gade, J.A. Chudasama, D.K. Parmar, H.D. Nakum, A.L. Patel, Spectrochem. Acta Mol. Biomol. Spectrosc. **140**, 174–184 (2015)
4. D.C. Crans, J.J. Smee, E. Gaidamauskas, L. Yang, Chem. Rev. **104**, 849–902 (2004)
5. V. Conte, B. Floris, Inorg. Chim. Acta **363**, 1935–1946 (2010)
6. G. Licini, V. Conte, A. Coletti, M. Mba, C. Zonta, Coord. Chem. Rev. **255**(19–20), 2345–2357 (2011)
7. T. Joseph, D. Srinivas, C.S. Gopinath, S.B. Halligudi, Catal. Lett. **83**(3–4), 209–214 (2002)
8. G. Barak, Y. Sasson, J. Chem. Soc. Chem. Commun. (16), 1266–1267 (1987)
9. N.S. Patil, B.S. Uphade, P. Jana, S.K. Bharagava, V.R. Choudhary, J. Catal. **223**(1), 236–239 (2004)
10. L. Nie, K.K. Xin, W.S. Li, X.P. Zhou, Catal. Commun. **8**(3), 488–492 (2007)
11. D.M. Gao, Q.M. Gao, Catal. Commun. **8**(4), 681–685 (2007)
12. M. Hüdlicky, *Oxidations in Organic Chemistry* (American Chemical Society, Washington, 1990)
13. J.E. Bäckvall (ed.), *Modern Oxidation Methods* (Wiley-VCH, Weinheim, 2004)
14. R.A. Sheldon, R.A. Van Santen, *Catalytic Axidation Applications* (World Scientific Publishing, Singapore, 1995)
15. A.K. Suresh, M.M. Sharma, T. Sridhar, Ind. Eng. Chem. Res. **39**(11), 3958–3997 (2000)
16. R. Alcántara, L. Canoira, P.G. Joao, J.M. Santos, I. Vázquez, Appl. Catal. A: Gen. **203**(2), 259–268 (2000)
17. K. Warangkana, T. Wimonrat, J. Met. Mater. Miner. **20**(2), 29–34 (2010)
18. M.R. Maurya, M. Kumar, U. Kumar, J. Mol. Catal. A: Chem. **273**(1–2), 133–143 (2007)
19. H. Klein, C. Kirschhock, H. Fuess, J. Phys. Chem. **98**(47), 12345–12360 (1994)
20. K.K. Bania, R.C. Deka, J. Phys. Chem. C **116**(27), 14295–14310 (2012)
21. W.H. Quayle, J.H. Lunsford, Inorg. Chem. **21**(1), 97–103 (1982)
22. W.H. Quayle, G. Peeters, G.L.D. Roy, E.F. Vansant, J.H. Lunsford, Inorg. Chem. **21**(6), 2226–2231 (1982)
23. M.S. Niasari, Z. Salimi, M. Bazarganipour, F. Davar, Inorg. Chim. Acta **362**, 3715–3724 (2009)
24. A. Sarkara, S. Pal, Inorg. Chim. Acta **361**, 2296–2304 (2008)
25. M.S. Niasari, Inorg. Chim. Acta **362**, 2159–2166 (2008)
26. M. Tsuchimoto, G. Hoshina, N. Yoshioka, J. Solid State Chem. **153**(1), 9–15 (2000)
27. J.C. Patrick, L.I. Sara, C.L. Sarah, J. Phys. Chem. A **105**(18), 4563–4573 (2001)
28. S.S. Dodwad, R.S. Dhamnaskar, P.S. Prabhu, Polyhedron **8**(13–14), 1748–1750 (1989)
29. S.N. Rao, D.D. Mishra, R.C. Maurya, N.R. Nageswara, Polyhedron **16**(11), 1825–1829 (1997)
30. L.J. Boucher, T.F. Yen, Inorg. Chem. **8**(3), 689–692 (1969)
31. K.K. Bania, R.C. Deka, J. Phys. Chem. C **115**(19), 9601–9607 (2011)
32. P.J. Carl, S.C. Larsen, J. Phys. Chem. B. **104**(28), 6568–6575 (2000)
33. B.R. Shaw, K.E. Creasy, C.J. Lanczycki, J.A. Sargeant, M. Tirhado, J. Electrochem. Soc. **135**(4), 869–876 (1988)
34. R. Zhang, J. Ma, W. Wang, B. Wang, R. Li, J. Electroanal. Chem. **643**(1–2), 31–38 (2010)
35. G.J. Alette, Ligtenbarg, H. Ronald, L.F. Ben, Coord. Chem. Rev. **237**(1-2), 89–101 (2003)